UPPSALA UNIVERSITY

INSTITUTE OF PHYSICS

Velocity- and Z-dependence of
transient magnetic fields in
ferromagnetic Gd

by

C. Fahlander, K. Johansson, E. Karlsson,
L.O. Norlin*and G. Possnert
Institute of Physics, University of
Uppsala, Box 530, S-751 21 Uppsala,
Sweden

UUIP-964 April 1977

Abstract

The ion-implantation perturbed angular correlation technique (IMPAC) was applied to the study of properties of Gd as stopping material. The transient magnetic fields at Fe, Ge, Mo, Ru, Pd, Cd and Te nuclei implanted into ferromagnetic Gd at 80 K were measured. The static magnetic hyperfine fields for Ru and Pd were deduced to be +65±25 kG and -45±23 kG, respectively. The Z_1-dependence could be fitted by the adjusted Lindhard-Winther theory except for the case of implanted Fe-nuclei. The deviating behaviour for the ^{56}Fe isotope was investigated in a separate experiment, where the dependence of the transient field was found to be directly proportional to the velocity of the recoiling ion. This result is in contradiction to the Lindhard-Winther model. Further consequences are discussed.

*Present address: CERN, Bat 577, EP division, Geneva, Switzerland

SW ISSN 0042-0263

Introduction

The ion-implantation perturbed angular correlation technique (IMPAC) [1,2] has during the last ten years been used extensively in investigation of internal hyperfine fields and nuclear moments. In the IMPAC method, Coulomb excitation and subsequent recoil implantation of a nucleus into a polarized ferromagnetic backing material is used to study the hyperfine interaction of excited nuclear states. The Larmor precession angle of the magnetic dipole moment of the excited level is determined by measuring the perturbed angular correlation between the emitted gamma-rays and the backscattered particles in a heavy ion beam. The excited nuclei are slowing down in the polarized backing and stopped within approximately 1 ps. During the stopping time the ions experience a transient magnetic field which is several megagauss in magnitude and parallel to the applied external field. The existence of a transient field at the nucleus during the slowing down process in ferromagnetic materials was first shown by Borchers et al. [3] for nuclei recoiling into iron.

For lifetimes of excited states less than a few ps, the precession of the magnetic dipole moments in the transient field may be greater than the precession in the static hyperfine field after stopping. This is especially the case for ions recoiling into Gd where the static hyperfine field in many cases can be neglected. The g-factor of the excited state may be obtained from the transient precession angle, (φ), provided a reliable calibration of the reduced transient shift (φ/g) exists for recoiling ions of the same kind.

Among the light nuclei ($A \leq 60$), the transient field effects in ferromagnetic iron were first used by Hubler et al. [4] to measure the magnetic moment of the shortlived 2+ state in ^{54}Fe (τ = 1.15 ps). The method was then subsequently applied to s-d shell nuclei by Eberhardt et al. [5,6]

and by Forterre et al. [7]. The results from these experiments are discussed in the framework of the linear response theory given by Lindhard and Winther [8].

In their theory the transient fields are proposed to originate from the scattering of polarized electrons by the attractive Coulomb field of the recoiling ion. Due to the enhancement of polarized electrons at the scattering center a large transient field can be expected. It was found that the predicted fields from the adjusted Lindhard-Winther (ALW) (see section 3) theory [9] could well reproduce the experimental data for elements with $Z \geq 26$ and for recoil velocities at $v/c \sim 1.6\%$.

However, recent experiments on light ions at high recoil velocities are in disagreement with the ALW theory. It was for instance found that the transient precession for ^{15}N recoiling into Fe at $v/c \approx 2\%$ was about a factor of 2 larger than that calculated from the ALW model [7]. New descriptions to explain these enhanced fields have been sought for. One such description is proposed by Eberhardt et al. [10] and is based on the idea of capture of polarized electrons from the ferromagnetic host into s-shell vacancies of the moving ion. This approach suggests that the transient field should be directly proportional to the recoil velocity in contrast to the ALW theory where an inverse proportionality is expected. The direct proportionality was also supported by an experiment where ^{56}Fe ions were allowed to recoil through various thicknesses of polarized iron and then stopped in Cu [11]. With such a procedure the contribution from the static field was eliminated and only the high velocity part of the transient precession was observed.

In the experiments performed until now Fe has most frequently been chosen as a ferromagnetic backing, but systematic studies have also been carried out with Co- and Ni-backings [12]. Much less theoretical as well as experimental work exists for Gd. The reason may be that the Gd metal has to be cooled to liquid nitrogen temperatures which complicates the measurements (see section 2.1). On the other hand, the number of polarized electrons per atom is a factor of three larger than in Fe which would imply that the transient field effect is enhanced a factor of two in Gd. Recent data [13,14] also confirm this assumption.

A more complete systematics is, however, needed in order to study the origin of the transient field (its dependence of velocity and atomic number Z_1 of the recoiling ion) and to be able to use it in measuring g-factors of excited states with lifetimes in the pico-second region.

In the present investigation of the Z_1 dependence of the transient field in Gd an enhanced field was observed in our experiment on the first 2^+ state in ^{56}Fe. A more detailed investigation with ^{56}Fe as a probe is therefore also reported.

2. Experiment

2.1. Experimental set-up

The IMPAC-equipment used in the present experiment at the EN tandem Van de Graaff accelerator in Uppsala has been described earlier [15]. Therefore, only the more pertinent aspects of the technique together with som new details on the equipment will be mentioned.

Beams of $^{16}O^{6+}$ ions with energies of 36 and 40 MeV were used to Coulomb excite and recoil implant the target nuclei into polarized ferromagnetic Gd. Coincidences between back-scattered particles and γ-rays following the Coulomb excitation process were collected. The particles were detected in a 300 μm thick annular surface barrier detector subtending angles between 165° and 175°. A typical particle spectrum is shown in Fig. 1. Four 3"x3" NaI (Tl) detectors were positioned at ±25° and ±115° with respect to the beam direction and at 10 cm distance from the target position. Due to the high symmetry in the experimental geometry systematic errors are minimized when averaging over complementary detectors.

The targets were positioned in an external magnetic field of 3.1 kG perpendicular to the detector plane. The field direction was automatically reversed after a preset amount of $2\cdot10^6$ particles in the particle window.

Gadolinium as a ferromagnetic host material for recoiling nuclei has not been used as extensively as iron in the IMPAC experiments. The reasons may be the more complex metallurgical properties of Gd as compared to iron and the fact that the Curie temperature is 293 K in Gd which means that the sample have to be cooled to liquid nitrogen temperature (~ 80 K) in order to be magnetized. A special cold finger was therefore constructed onto which the target was mounted. The target will, however, act as a cold trap when cooled to 80 K and special precautions to prevent build up of dirt and moisture had to be taken. By surrounding the target with a cold cap of aluminium the cold area inside the chamber was increased. The vacuum was improved and a pressure of better than 10^{-6} Torr was achieved. Furthermore, accumulated radiation damage as well as build up of dirt were avoided by changing and heating the target every 6 hours.

A cross section of the scattering chamber showing the cold finger and the pole pieces of the electromagnet is displayed in Fig. 2. The iron tubes along the beam line are shielding the beam from the fringing field of the magnet.

2.2 Targets

The targets were prepared from isotopically enriched material except for the case of the Ge isotopes where measurements on natural Ge were performed. The thicknesses of the targets were ~ 100-400 $\mu g/cm^2$ and the material were sputtered or evaporated onto ~ 0.025 mm thick Gd backings. A thin layer of indium were pressed between the Gd foil and a Cu layer of thickness 0.1 mm to ensure good thermal contact between the target and the copper heat sink.

The magnetizing properties of the Gd foil were studied in a magnetometer measurement and the result is presented in Fig. 3. As can be seen, the external field of 3.1 kG was sufficient to saturate the foils up to 90%. Skaali et al. [14] have investigated the dependence of the precession angle on the applied field. No reduction of the total precession angle above a polarizing field of 1 kG was observed.

2.3. Experimental conditions

In order to reduce radiation damage and heating effects the beam current never exceeded 50 nA. This seems to be a reasonable limit, since no significant variation was found in the mean precession angle, when the current was below 60 nA. Special care has been taken with the cooling system. A beam of 50 nA 40 MeV $^{16}O^{+6}$ will transfer a power of 0.2 W to the target and if the heat transport is insufficient this will decrease the magnetization of the Gd backing. To check the heat transport capacity of the actual target assembly, a special experiment with higher current (150 nA) was carried out where a thermocouple was mounted on the target at beam spot position. Under the beam conditions mentioned above no changes in the macroscopic temperature was observed.

The fringing field from the polarizing magnet bends the trajectories of both incoming and scattered particles. This results in a shift of the polar axis z which is detected as a precession of the correlation pattern. In order to evaluate the true precession from the total mean shift, the beam bending was determined from a separate experiment where ^{110}Pd was implanted into a Cu backing. The effect was found to be 4.5 ± 1.0 mrad and 1.6 ± 1.5 mrad for $^{16}O^{+6}$ at 36 and 40 MeV respectively.

2.4. Stopping power measurement

During the course of our investigations, there arose an interest in studying the transient magnetic effect at different velocities of the recoiling ion (see section 3).There are two possible ways to vary the energy of ions entering the backing material, namely by changing the incoming beam with respect to mass or energy or by letting the recoils pass through a degrader material before entering the backing.

The use of a degrader between the target and the backing allows one to reach low velocities still maintaining a high Coulomb excitation yield, but it requires quite an accurate value of the stopping power. Very few experimental data exist on heavy ions ($Z > 26$) in high-Z elemental solids. The actual energy distribution of Fe ions at 25 MeV after passing through Cu-layers of various thicknesses have therefore been measured.

The experimental set up (Fig. 4a) consists of two movable silicon surface barrier detectors, number 2 for detection of the recoil and number 1 for discriminating non-coincident scattered events. The recoil velocity can then be changed either by varying the entrance energy of the beam or by changing the detection positions. The results presented in Fig. 4b and table 1 agrees with interpolated values from the tabulations of Northcliffe and Schilling [16].

2.5. Data Collection

The electronic system is based on the usual fast-slow coincident arrangement (Fig. 5). The coincident γ-rays were routed and stored in a LABEN 4096 multichannel analyzer. The total coincidence spectra were recorded in the first eight subgroups of the MCA memory and the random ones in the second half. Spectra corresponding to field "up" and "down" were automatically stored in even and odd subgroups respectively. The data were regularly dumped on magnetic tapes and immediately analyzed on a PDP-15 computer. An example of a coincidence spectrum is shown in Fig. 6.

Particles scattered from targets with $A < 170$ can not be discriminated from particles originating from the Gd backing and therefore γ-rays from Gd will also be present in the coincidence spectra. This is, however, in most cases no problem since the Gd γ-ray energies are below 300 keV. The particle spectrum was continously monitored on a separate multichannel analyzer to check the particle gate.

2.6. Data analysis

The number of true coincidences $C(\theta,\pm B)$ accumulated in the γ-detectors positioned at angles θ with respect to the beam were obtained from the photopeak intensities after a correction for accidental events and a background subtraction. From the number of coincidences recorded in up (+B) and down (-B) field respectively the ratio

$$R = \frac{C(\theta,+B)-C(\theta,-B)}{C(\theta,+B)+C(\theta,-B)}$$

was formed from which the precession angle $\Delta\theta$ was determined. Since this angle is small ($\Delta\theta \ll 1$) the following approximation holds

$$R \approx \frac{1}{W}\frac{dW}{d\theta}(\Delta\theta)$$

where W is the time integral angular correlation function. In our case, where both a transient ($\varphi(t)$) and a static magnetic perturbation are present W consists of two parts namely

$$\overline{W(\theta,B,\infty)} = \frac{1}{\tau}\int_0^{t_s} e^{-t/\tau} W(\theta-\varphi(t))dt + e^{-t_s/\tau} W(\theta-\varphi(t_s)-\omega_s\tau)$$

where t_s is the stopping time of the recoiling ion and τ is the lifetime of the nuclear level under study. The quantity ω_s is the Larmor frequency in the static field. In the next section a short summary of the theoretical models used for the interpretations of the experimental data will be given.

3. Transient magnetic fields

The total angular shift ϕ through which a nuclear magnetic moment rotates in a time t, when placed in a magnetic field B(t) will be expressed by the integral

$$\phi(t) = g\frac{\mu_N}{\hbar}\int_0^t B(t)dt \qquad (1)$$

where μ_N is the nuclear magneton and g the gyromagnetic ratio of the nuclear level.

The first theoretical model for the time depencence, B(t), was given by Lindhard and Winther [8]. They proposed the field to originate from the Fermi contact interaction whose average value in Gd would correspond to a field

$$B = \frac{8\pi}{3} \mu_B N\delta \tag{2}$$

where μ_B is the Bohr magneton, N is the atomic density, and δ is the number of polarized electrons per atom. For a saturated Gd sample at 80 K, δ is approximately 7 and an average hyperfine field on Gd of 40 kG is expected. For an ion moving with velocity v_r the density of scattered polarized electrons is enhanced at the positively charged ion. By solving the nonrelativistic Schrödinger equation for an unscreened Coulomb potential the enhancement factor was obtained as

$$\chi = 2\pi Z_1 \frac{v_0}{v_r} \tag{3}$$

where v_0 is the Bohr velocity, and Z_1 is the atomic number of the ion. From this theory the enhancement is expected to be inversely proportional to the ion velocity, which means that the field reaches a maximum just before the ion comes to rest.

The magnitude of χ can be estimated by putting $v_r = v_0$ which implies a transient magnetic field of ~ 10 MGauss for Fe recoiling into Gd. By averaging over the velocity of the polarized electrons and taking relativistic (R) as well as atomic resonance and binding effects (P·C) into account the following expression for the magnetic field is derived:

$$B(v) = \frac{16\pi^2}{3} \mu_B N\delta RPCZ_1 \left(\frac{v_0}{v_p}\right) f(v) \tag{4}$$

$$f(v) = \begin{cases} v_p/v & v > v_p \\ 1 & v < v_p \end{cases}$$

where v_p is the effective velocity of the polarized electrons. The function B(t) can be obtained from B(v) by use of the stopping power relation, v(t). The reduced transient field effect φ/g obtained by integration of eq. 1 with B(v) given by eq. 4 was found to be a factor of two below the experimental results. The model was however adjusted (ALW) by Hubler et al. [9] who fitted the parameter v_p to the existing data. It was then possible to reproduce the Z_1-dependence of the transient effect for $Z_1 \gtrsim 26$.

In recent experiments on the velocity dependence of B(v) carried out with light elements recoiling into iron the results were twice as large as expected even from the adjusted theory. In the paper by Eberhardt et al. [10] on Si recoling into Fe an empirical expression

$$B(v) = aRZ_1 \left(\frac{v}{v_0} \right)^p \tag{5}$$

was instead proposed and with a=12.5±1.7 T and p=1.05±0.25 they could reproduce the experimental data. They interpreted the large transient fields to arise from capture of polarized electrons into bound orbitals of the moving ion.

The measured rotaion $\Delta\theta$ is a combined effect of the transient precessioh φ and a precession in the static field (B_{stat}) which is assumed to take place after the ion has come to rest. For short lived states ($\tau \lesssim t_s$) a correction for decay in flight has to be taken into account. The final analytical expressions (valid for small $\Delta\theta$) that have been used in the interpretation of the experimental data are then

$$\Delta\theta_{meas} = -g \left\{ \frac{\mu_N}{\hbar} \tau B_{stat} e^{-t_s/\tau} - \frac{\varphi(\tau)}{g} \right\} \tag{6}$$

$$\frac{\varphi(\tau)}{g} = \frac{\mu_N}{\hbar} A_1 M \int_0^v \frac{B(v) e^{-t(v)/\tau}}{dE/dR} \, dv \tag{7}$$

A_1M is the mass of the moving ion and dE/dR is the stopping power of the backing material. For details see appendix.

4. Results

In analyzing our results according to ALW-theory with the parameters taken from ref. 14 an anomalous field was found for ^{56}Fe. The transient angular shift was a factor of two larger than the predicted one and a detailed investigation for this case was therefore carried out with respect to the velocity dependence of the field. Since the hyperfine magnetic field for Fe in Gd is close to zero [17] only a transient effect is present. Furthermore the correction for decay in flight can be neglected since the lifetime of the 2_1^+ state in ^{56}Fe is fairly long ($\tau \approx 10$ ps).

The Fe nuclei were excited by a beam of $^{16}O^{6+}$ ions of 36 MeV implying a maximum recoil energy of 25 MeV. The entrance velocity of the ions recoiling into the ferromagnetic backing were varied by making use of a Cu degrader between the target and the backing (see section 2.4).

The results presented in Fig. 7 and Table 1 show a velocity dependence which is in contradiction to the ALW-theory. The dependence is closer to the linear type found by Eberhardt et al. [10] for Fe backings. It is therefore reasonable to use the empirical expression (eq. 5) also in the Gd case. With p=1, the parameter a in this equation was deduced from the measurements on Ru and Pd isotopes presented in Table 2. For these long-lived isotopes the transient shift φ can be extracted quite accurately since the static precession as well as the g-factor are well known from radioactive work. From the extracted φ and eq. 7 a value of $a=12.6\pm0.6$ T was obtained. With the parameters given above, φ/g is calculated as a function of initial recoil velocity (proportional to $\sqrt{E}$) for ^{56}Fe and presented in Fig. 7 by a solid line. The parameter a in the empirical expression (eq.5) is found to be equal for Gd- and Fe backings. The reason for this may be that the number of polarized electrons per unit volume is almost the same for the two metals which implies mean magnetic fields (eq.2) of the same order. The longer stopping time in Gd (t_s(Gd)~2.5 ps; t_s(Fe)~1 ps) will explain the larger transient effect in this metal.

In the Z_1-systematics of φ/g in Gd (Fig. 8) the effect of the new empirical B(v) relation has been taken into account by use of equation (7) for all available experimental data. It mainly affects the data for Ge and Te ions. The values of φ/g displayed in the figure are normalized to $\tau=\infty$ and $v/v_0 = 4.0$. The measured total angular shifts $\Delta\theta$ corrected for beam bending are presented in Table 3 together with the nuclear parameters used in the analysis for the isotopes investigated. It was not possible to extract the static fields, B_{stat}, and have meaningful results except for Ru and Pd nuclei (Table 4). In these cases the nuclear lifetimes are long enough and sufficiently separated to make it possible to determine B_{stat} accurately enough. The results for RuGd and PdGd are +65±25 kGauss and -45±23 kGauss, respectively in good agreement with radioactive measurements [18,19]. Fig. 9 displays the experimental precessions as function of the lifetime of these isotopes. The slope of the dashed lines corresponds to the static fields calculated with average g-factors and the intercept at $\tau=0$ represents the transient angular shift.

5. Conclusion

It is obvious from existing data that the transient fields are quite complex in their nature. An ion traversing a solid material is subject to several processes which might be reflected in the transient shifts. The present experiment on transient shifts in Gd are consistent with a directly proportional velocity dependence in accordance with the recent data for recoils in ferromagnetic Fe. Therefore, the mechanism of Lindhard and Winther can not alone describe the phenomena (but may still give a contribution to the transient magnetic effect). The main part of the interaction for high energy recoils seems to have another origin. One possible description of the effects might be found in the fundametal processes of electron pick-up and shake-off during the stopping. In order to explain the large transient fields with such a microscopic model the polarized electrons have to be captured into vacancies in the inner bound s-shells of the ion. Such a pick-up of electrons can be achieved through several channels and at this stage the experimental results can only be discussed from a qualitative point of view. The phenomenological approach by Eberhardt et al. [10] seems to reproduce the experimental results fairly well also for gadolinium as a stopping material.

One immediate consequence if the linear velocity dependence of B(v) is accepted is that earlier IMPAC data on the g-factors of the most short-lived nuclear states must be re-evaluated. Another consequence is that the use of high energy recoils may extend the number of possible g-factor measurements down into the sub-pico-second region. It would therefore be of interest to perform further experiments on the details of the transient fields, especially at velocities higher than those used in the present investigation.

Appendix

A more detailed outline of the analytical formulas used in the numerical calculations will be given together with examples of physical cosequences.

The energy E (keV) and range R (m) have been transformed to the dimensionless variables ε and ρ [22].

$$\varepsilon = 32.527 \frac{A_2 Z^{-1/3}}{Z_1 Z_2 (A_1+A_2)} E \qquad \text{(A1)}$$

$$\rho = 1.661 \cdot 10^6 \frac{A_1 Z^{-2/3}}{(A_1+A_2)^2} \rho' R \qquad \text{(A2)}$$

$$Z = (Z_1^{2/3} + Z_2^{2/3})^{3/2}$$

where ρ' is the density of the stopping media (g/cm^3). $Z_{1,2}$ and $A_{1,2}$ are the atomic and mass numbers for the ion and host (subscript 1 and 2) respectively. This transformation has been performed to describe the stopping at low velocities conveniently (see below).

In the estimates of the transient magnetic field precession from the Lindhard and Winther theory the following expressions have been used:

$$\varphi/g = 2.209 \cdot 10^{-6} \, qR\delta C\left(\frac{v_0}{v_p}\right) I(v) \qquad \text{(A3)}$$

$$q = \left(\frac{Z Z_1 (A_1+A_2)^3}{Z_2 A_1 A_2}\right)^{1/2}$$

$$R \cong 1 + \left(\frac{Z_1}{84}\right)^{2.5}$$

$$I(v) = \int_{\varepsilon_0}^{\varepsilon_p} \frac{e^{-t(\varepsilon)/\tau} d(\varepsilon^{1/2})}{d\varepsilon/d\rho} + \int_{\varepsilon_p}^{\varepsilon} \left(\frac{\varepsilon_p}{\varepsilon}\right) \frac{e^{-t(\varepsilon)/\tau} d(\varepsilon^{1/2})}{d\varepsilon/d\rho} \qquad \text{(A4)}$$

R is here an approximate correction for relativistic effects. The stopping power $d\varepsilon/d\rho$ arises from a $dt \rightarrow d\varepsilon$ transformation of eq.1. The number of polarized electrons δ and their effective velocity v_p depend on the backing used and are together with C input parameters in the numerical calculations. C takes care of the atomic effects of the host atoms and the moving ions. To correct for decay in flight of excited states with short life time the stopping time $t(\varepsilon)$ has to be known. From ref. 22 one derives:

$$t(\varepsilon) = \frac{7.816\cdot 10^{-16}}{\rho'} \left\{ \frac{A_2}{A_1} \frac{(A_1+A_2)^3 Z}{Z_1 Z_2} \right\}^{1/2} \int_{\varepsilon_i}^{\varepsilon} \frac{d\varepsilon}{\varepsilon^{1/2} d\varepsilon/d\rho} \qquad \text{(A5)}$$

where ε_i corresponds to the initial (entrance) energy of the ion.

In order to evaluate the integrals A4 and A5 an analytical expression of the specific energy loss $d\varepsilon/d\rho$ is needed. The comprehensive formulas given by Lindhard, Scharff and Schiøtt [22] have been used here:

$$d\varepsilon/d\rho = s_n + s_e \qquad \text{(A6)}$$

$$s_e = k \cdot \varepsilon^{1/2}$$

$$k = 0.0793\ \xi_e \frac{Z_1^{1/2} Z_2^{1/2} (A_1+A_2)^{3/2}}{Z^{1/2} A_1^{3/2} A_2^{1/2}}; \qquad \xi_e \cong Z_1^{1/6}$$

s_n is the nuclear stopping which reaches a maximum during the end of the path and s_e corresponds to the electronic stopping. This approximation yields values to within 20% accuracy, which is sufficient for the purpose of the present work. For refined calculations, however, the data in ref. 16 and 23 can be used or special measurements be performed.

With use of the LSS-stopping A4 was numerically integrated. The results for ^{56}Fe recoiling into Gd at diffrent energies and with assumed lifetimes of 1 ps and 10 ps respectively, are displayed in Fig. 10. In this figure ALW corresponds to one set of parameters given by Skaali [14] and LW to the non-adjusted model. In the same figure (full line) the integrated effect from a field of the form given by eq. 5 is shown. It is seen that φ/g for a direct velocity dependence of the transient field is less sensitive for decay in flight which is favourable in g-factor measurements of short lived nuclear states.

The calculated stopping time in Gd (eq. A5), for heavier elements ($Z_1 \geq 26$) at medium recoiling energies, are between 1.5 ps and 2.5 ps (Fig. 11). For excited states with lifetimes comparable to the stopping time a reduction of the static rotation with 30% is implied. Due to the large transient field in Gd the effect from the static part will provide no more than 5% of the total precession. From this one can conclude that the effect of radiation damage is negligible when Gd is used as a backing material, since the transient magnetic fields are only slightly affected by radiation damage [9].

Acknowledgement

We are indepted to Prof. A. Johansson and the staff at the Tandem Laboratory for providing good research conditions.

The authors also want to thank Mr. L. Einarsson and Mr. J. Kjellberg for their skillful preparation of the targets.

We are also grateful to Dr. L. Lundgren for performing the magnetometer measurements.

This work was financially supported by AFR.

References

1. L. Grodzins, in Nuclear Reactions Induced by Heavy Ions edited by R. Bock and W.R. Hering (North-Holland Amsterdam, 1970) p. 367

2. R.R. Borchers, in Hyperfine Interactions in Excited Nuclei edited by G. Goldring and R. Kalish (Bordon and Breach, New York, 1971), Vol. 1, p. 31

3. R.R. Borchers, B. Herskind, J. Bronson, L. Grodzins, R. Kalish and D.E. Murnick, Phys. Rev. Lett. 20 (1968) 424

4. G.K. Hubler, H.W. Kugel and D.E. Murnick, Phys. Rev. Lett. 29 (1972) 662

5. J.L. Eberhardt, R.E. Horstman, H.W. Heeman and G. van Middelkoop, Nucl. Phys. A229 (1974) 162

6. J.L. Eberhardt, R.E. Horstman, H.A. Doubt and G. van Middelkoop, Nucl. Phys. A244 (1975) 1

7. M. Forterre, J. Gerber, J.P. Vivien, M.B. Goldberg, K.-H. Speidel and P.N. Tandon, Phys. Rev. C11 (1975) 1976

8. J. Lindhard and A. Winther, Nucl. Phys. A166 (1971) 413

9. G.K. Hubler, H.W. Kugel and D. Murnick, Phys. Rev. C9 (1974) 1954

10. J.L. Eberhardt, R.E. Horstman, P.C. Zalm, H.A. Doubt and G. van Middelkoop, to be published in Hyperfine Interactions

11. M. Hass, J.M. Brennan, H.T. King, K. Saylor and R. Kalish, Phys. Rev C14 (1976) 2119

12. D.E. Murnick, in Angular Correlations in Nuclear Disintegration, edited by H.van Krugten and B. van Nooijen (Rotterdam University Press, 1971) p. 455

13. K. Johansson, L.-O. Norlin, G. Possnert and E. Karlsson, Hyperfine Interactions 2 (1976) 212

14. B. Skaali, R. Kalish and B. Herskind, Hyperfine Interactions 1 (1976) 381

15. K. Johansson and L.-O. Norlin, UUIP-866 (1974), Institute of Physics, Uppsala

16. L.C. Northcliffe and R.F. Schilling, Nuclear Data Tables 7 (1970) 233

17. W.D. Brewer and E. Wehmeier, Phys. Rev. B12 (1975) 4608

18. L. Boström, G. Liljegren, B. Jonsson and E. Karlsson, UUIP-742 (1971)

19. L. Boström, K. Johansson, E. Karlsson and L.-O. Norlin, see ref. 2, vol. 2 p. 466

20. L. Boström, B. Jonsson, G. Carlsson and E. Karlsson, Physica Scripta 3 (1971) 183

21. M. Pasternak, Phys. Lett. A32 (1970) 449

22. J. Lindhard, M. Scharff and H.E. Schiøtt, Mat. Fys. Medd. Dan. Vid. Selsk. 33 no 14 (1963)

23. W.M. Curry, Nucl. Instr. 73 (1969) 173

24. G.M. Heestand, P. Hvelplund, B. Skaali and B. Herskind, Phys. Rev. B2 (1970) 3698.

Table captions

Table 1. Reduced transient magnetic field on ^{56}Fe implanted into ferromagnetic Gd at different velocities. For the first excited 2^+ state of 847 keV a lifetime τ = 9.67(29) ps and a g-factor of g = 0.60(10) has been used.

Table 2. Experimental results for Ru and Pd implanted into ferromagnetic Gd together with nuclear parameters used in the analysis.

Table 3. Experimental results for Ge, Mo, Cd and Te implanted into ferromagnetic Gd together with nuclear parameters used in the analysis.

Table 4. Reduced transient shifts and static magnetic fields at even nuclei in ferromagnetic Gd(T = 77 K).

Figure captions

Fig. 1. A particle spectrum of 36 MeV $^{16}O^{6+}$ ions back-scattered from a 200 μg/cm^2 thick Ge target on a Gd backing.

Fig. 2. Simplified sketch of the IMPAC scattering chamber showing the cold finger carried down through (thermally and electrically insulated) the upper pole piece of the electromagnet.

Fig. 3. Magnetometer measurements of a Gd foil. The average number of Bohr magnetons per atom is plotted as a function of the applied field.

Fig.4a. Experimental setup for the stopping power measurement.

Fig.4b. Energy loss of ^{56}Fe passing through Cu layers of various thicknesses.

Fig. 5. A coincidence γ-spectrum for a natural Ge target.

Fig. 6. A block diagram of the IMPAC electronic setup. The system records the total and the accidental coincidences simultaneously on LABEN multichannel analyser.

Fig. 7. Measured reduced transient shifts for ^{56}Fe recoils as a function of the square-root of the recoil energy. The line labeled LW corresponds to calculations within the Lindhard and Winther model and ALW to the adjusted model with the parameters $v_p = 0.18\ v_o$ and $C = 1.0$ taken from ref. 14. The solid line is calculated using the empirical formula of B(v) (eq. 5) with the parameters obtained in the present work.

Fig. 8. All available reduced transient field data in Gd vs Z_1. The displayed values are normalized to $\tau = \infty$ and a recoil velocity $v/v_0 = 4.0$. The reduced transient shifts of Yb, Gd and Sm are taken from ref.14 and Pt from ref. 24. The Cd point represent a weighted meanvalue of the result from the present work and that of ref. 14.

Fig. 9. IMPAC values $\Delta\theta$ vs meanlife for Pd and Ru implanted into Gd.

Fig.10. Theoretical calculations of reduced transient shifts for ^{56}Fe recoiling into Gd at different energies and with assumed lifetimes of 1 ps and 10 ps respectively. The same parameters are used as in Fig. 7.

Fig.11. Predicted values of the stopping time (eq. A5) for Fe, Cd and Pt as a function of the recoil energy.

Table 1.

Cu degrader mg/cm^2	$E_{entrance}$ MeV	v/v_o	$-\omega\tau$ mrad	$-\varphi/g$ mrad
0	24.51	5.06	34.9±5.1	57±15
0.8	12.25±0.75	3.58±0.22	15.3±4.2	26±6.8
1.8	5.40±0.75	2.38±0.33	9.6±3.5	16±6.4

Table 2.

Nucl	2^+ keV	E_r MeV	v/v_o	τ ps	g	$-\omega\tau$ mrad
^{102}Ru	475	18.62	3.96	23.1±1.4	0.41±0.03	33.5±1.5
^{104}Ru	358	18.39	3.92	77.9±5.8	0.41±0.05	40.5±1.0
^{106}Pd	512	18.10	3.88	17.3±1.2	0.40±0.03	25.5±1.4
^{108}Pd	434	17.87	3.84	34.3±2.5	0.36±0.02	22.2±1.4
^{110}Pd	374	17.64	3.81	62.0±4.3	0.35±0.03	21.2±1.4

Table 3.

Nucl	2^+ keV	E_r MeV	v/v_o	τ ps	g	$-\omega\tau$ mrad
^{72}Ge	834	21.11	4.47	4.76±0.58	0.37±0.10	17.7±1.9
^{74}Ge	596	20.84	4.41	18.80±0.29	0.35±0.08	20.3±1.3
^{98}Mo	787	19.08	4.04	5.0 ±0.6	0.34±0.18	23.5±2.3
^{100}Mo	536	18.88	4.00	14.9 ±1.6	0.34±0.18	23.4±1.6
^{110}Cd	658	17.57	3.81	7.2 ±0.7	0.35±0.07	23.5±3.6
^{116}Cd	513	16.92	3.71	19.8 ±1.4	0.41±0.11	15.2±3.2
^{122}Te	564	16.27	3.62	11.0 ±1.6	0.39±0.16	24.8±2.0
^{124}Te	603	16.06	3.59	9.5 ±0.6	0.44±0.06	19.0±2.6
^{126}Te	743	15.64	3.53	4.6 ±0.6	0.35±0.07	17.0±2.0

Table 4.

Nucl	$-\varphi/g$ mrad	B_{stat} (k Gauss) IMPAC present work	RAD	
Fe	43±11		0±16	a)
Ge	43±16			
Mo	71±20			
Ru	75±10	+65±25	+50±10	b)
Pd	76±5	-45±23	-64±6	c)
Cd	76±38		-312±9	c)
Te	76±40		-33±10	d)
			-229±2	e)

a) ref. 17
b) ref. 18
c) ref. 19
d) ref. 20
e) ref. 21

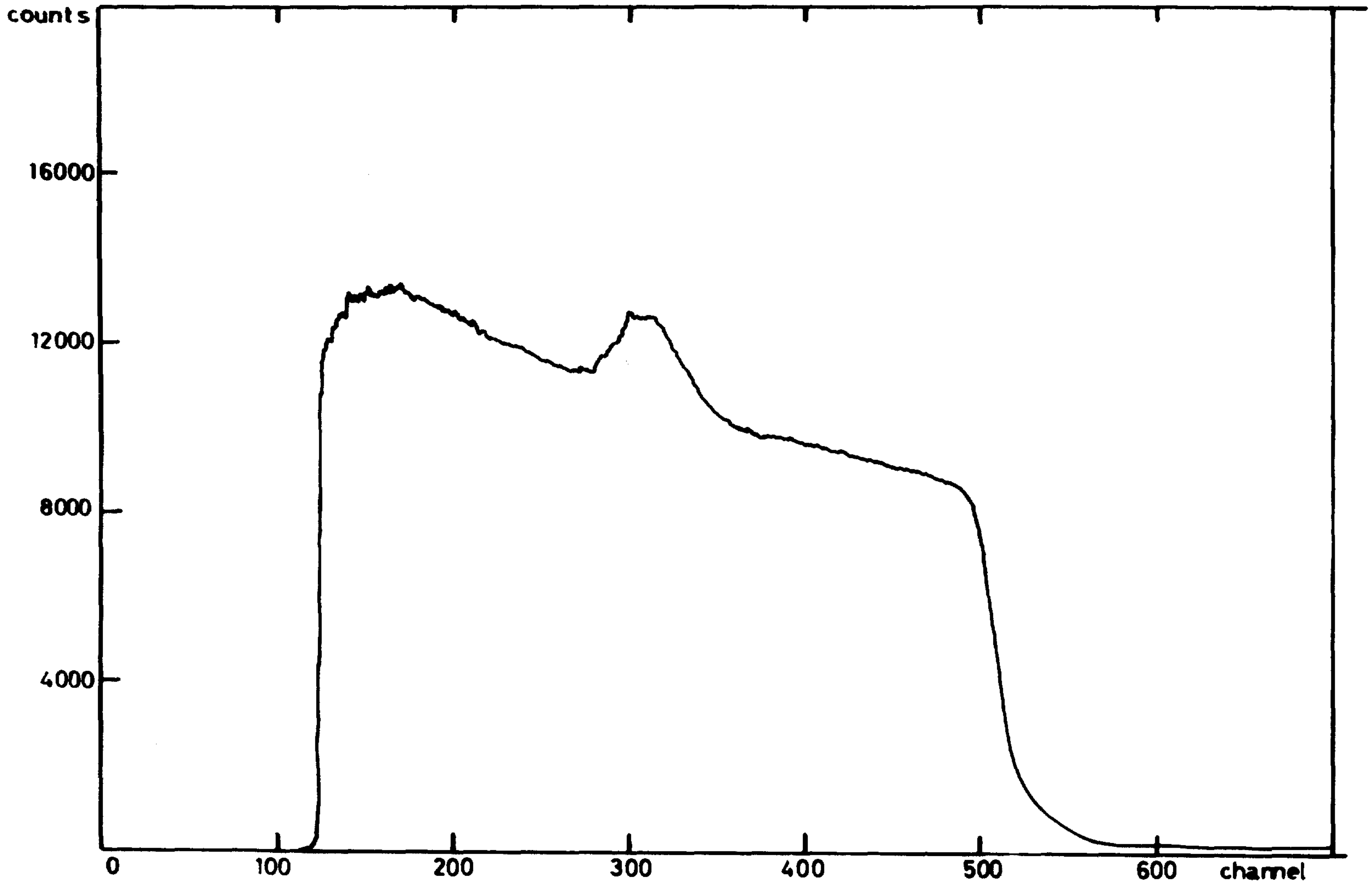
counts
16000
12000
8000
4000
0
100
200
300
400
500
600
channel

FIG 1

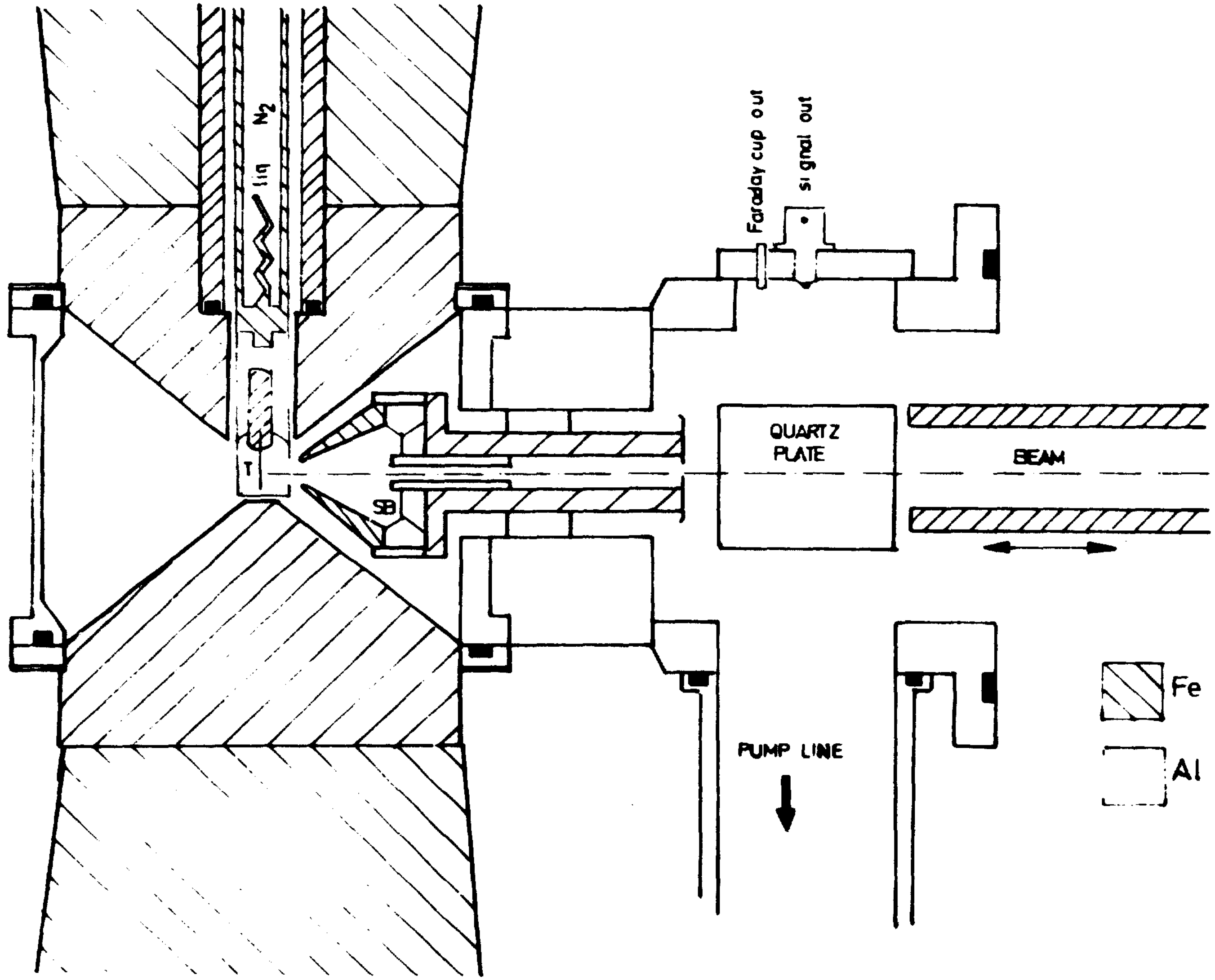
liq N_2
Faraday cup out
si gnal out
T
SB
QUARTZ PLATE
BEAM
PUMP LINE
Fe
Al

FIG 2

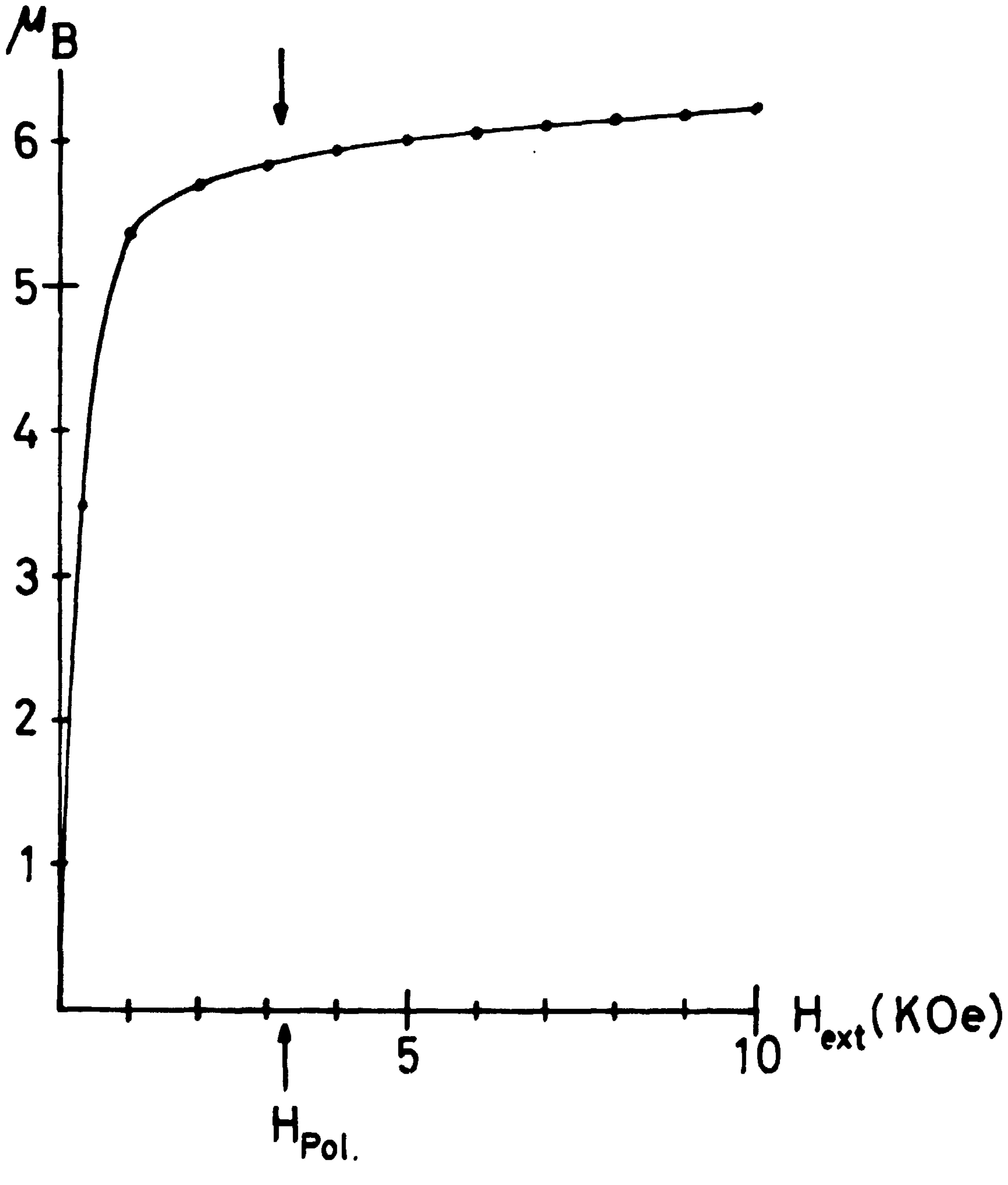

FIG 3

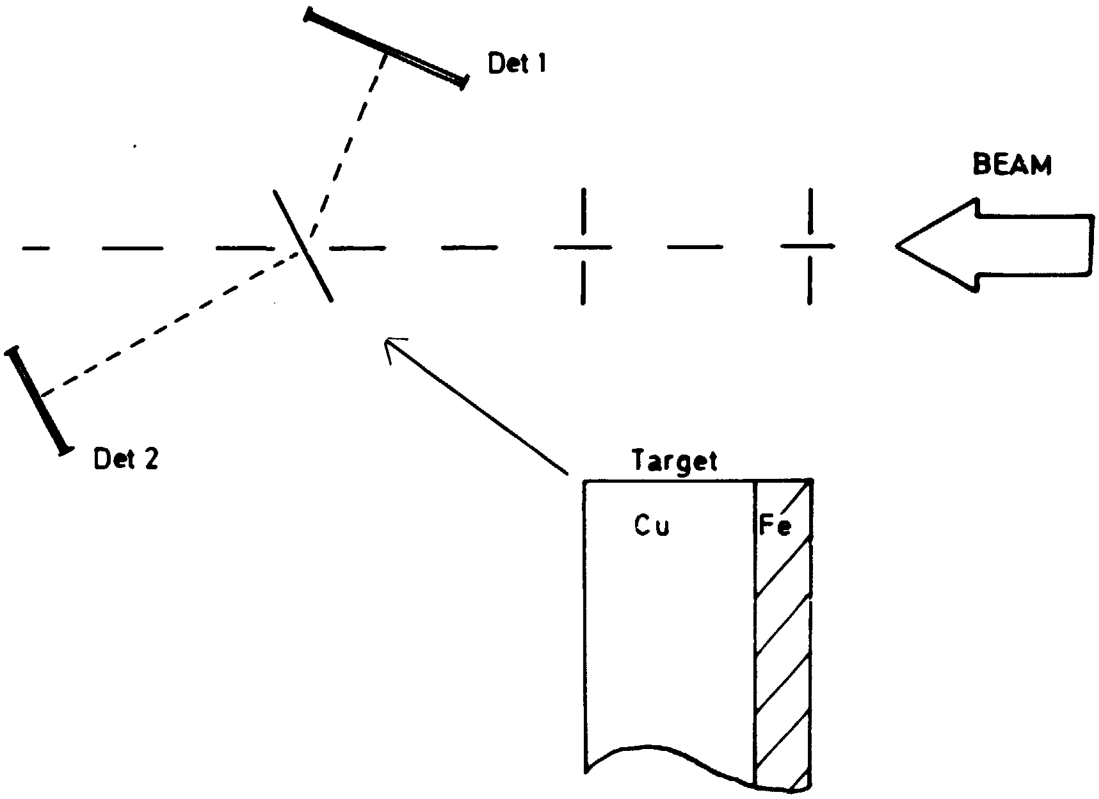

FIG 4a

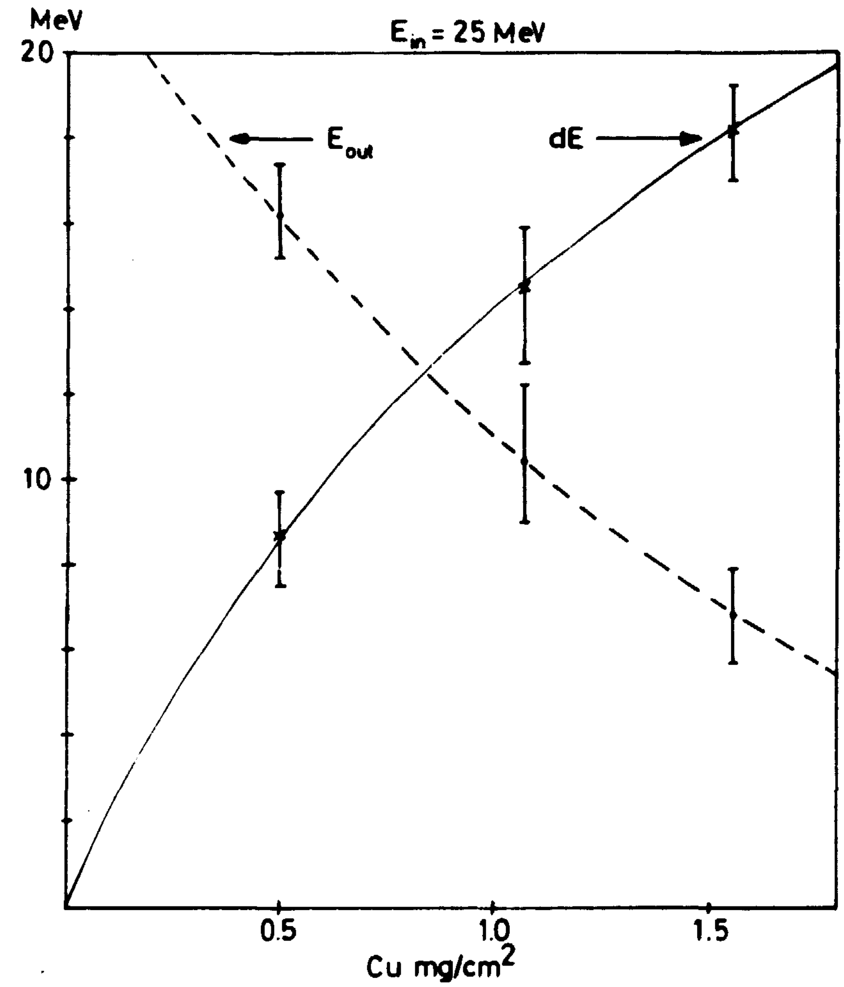

FIG 4b

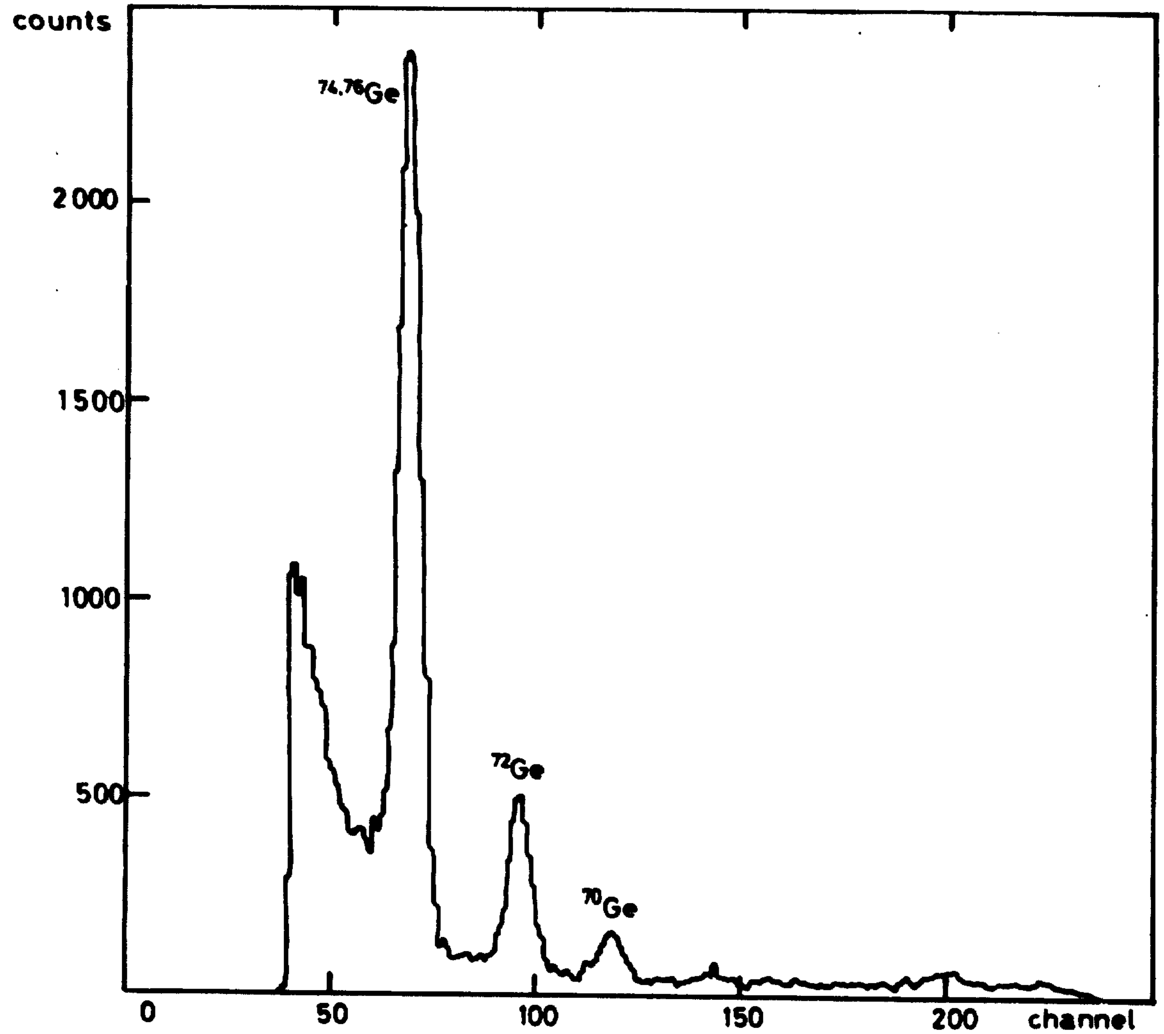
counts
2000
1500
1000
500
0
50
100
150
200
channel
$^{74,76}Ge$
^{72}Ge
^{70}Ge

FIG 5

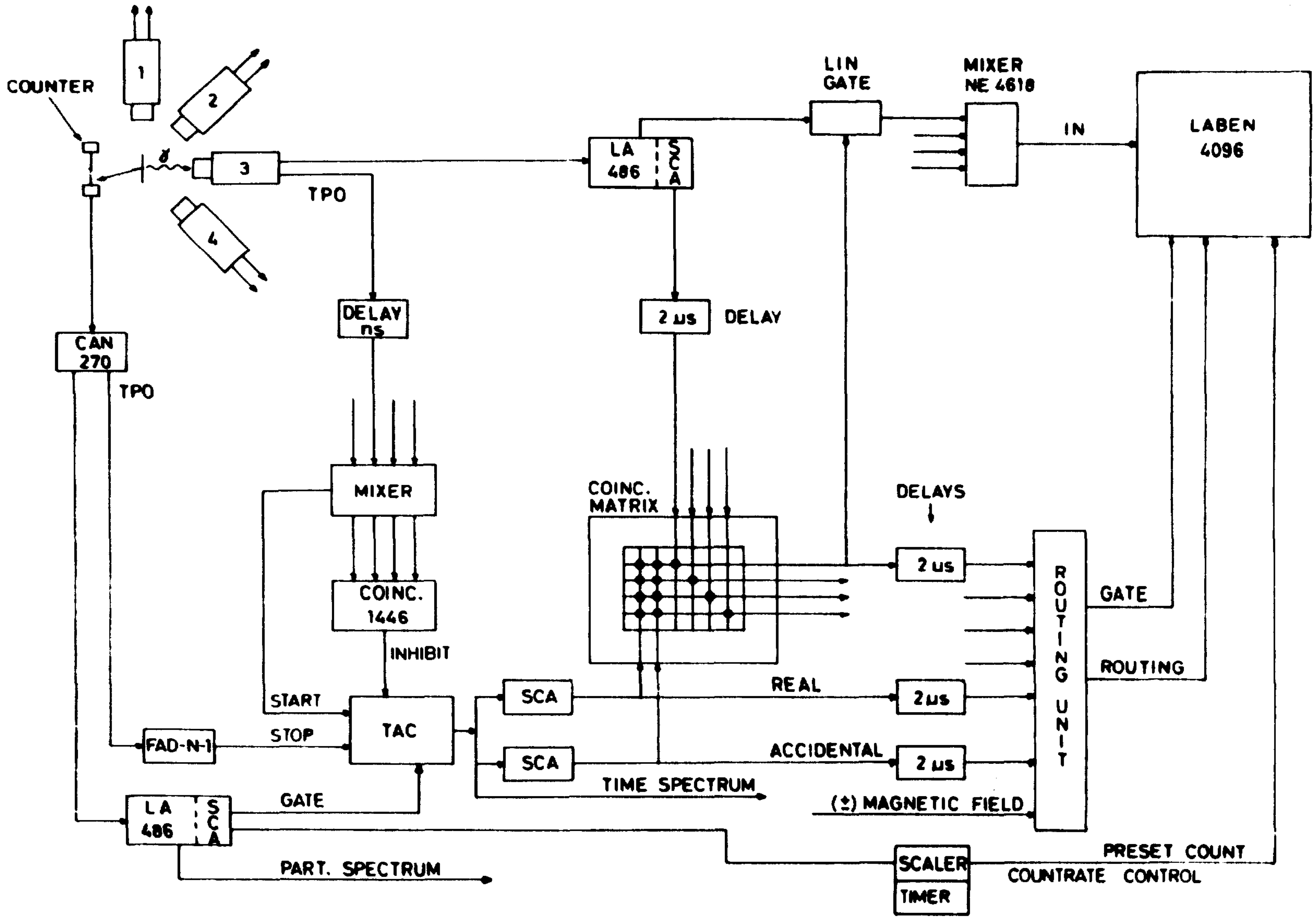
COUNTER
1
2
3
4
TPO
CAN 270
TPO
DELAY ns
MIXER
COINC. 1446
INHIBIT
START
STOP
FAD-N-1
TAC
GATE
LA 486 SCA
PART. SPECTRUM
LA 486 SCA
LIN GATE
MIXER NE 4618
IN
LABEN 4096
2 µs DELAY
COINC. MATRIX
DELAYS
2 µs
SCA
SCA
REAL
ACCIDENTAL
2 µs
2 µs
TIME SPECTRUM
(±) MAGNETIC FIELD
ROUTING UNIT
GATE
ROUTING
SCALER
TIMER
PRESET COUNT
COUNTRATE CONTROL

FIG 6

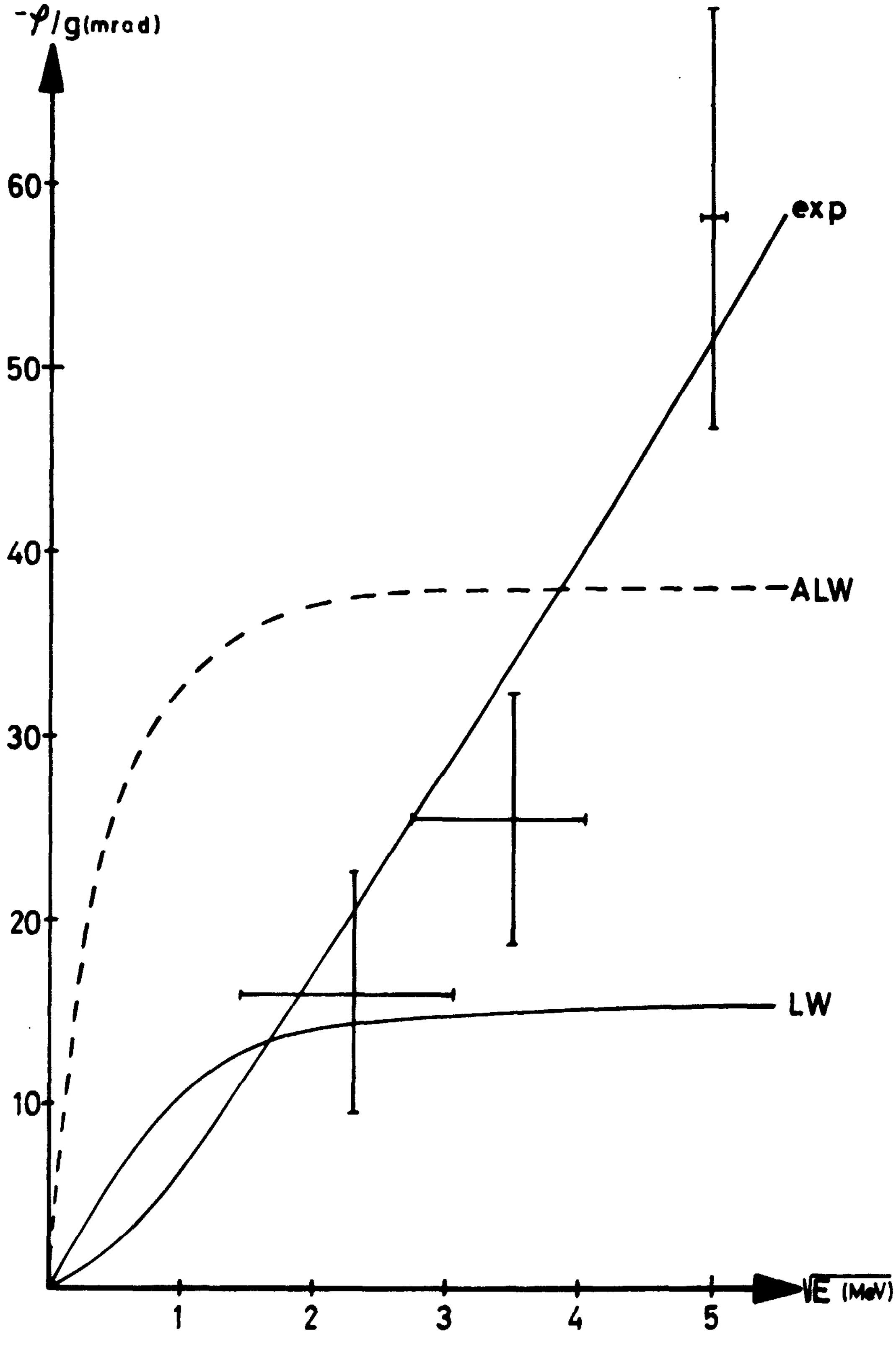

FIG 7

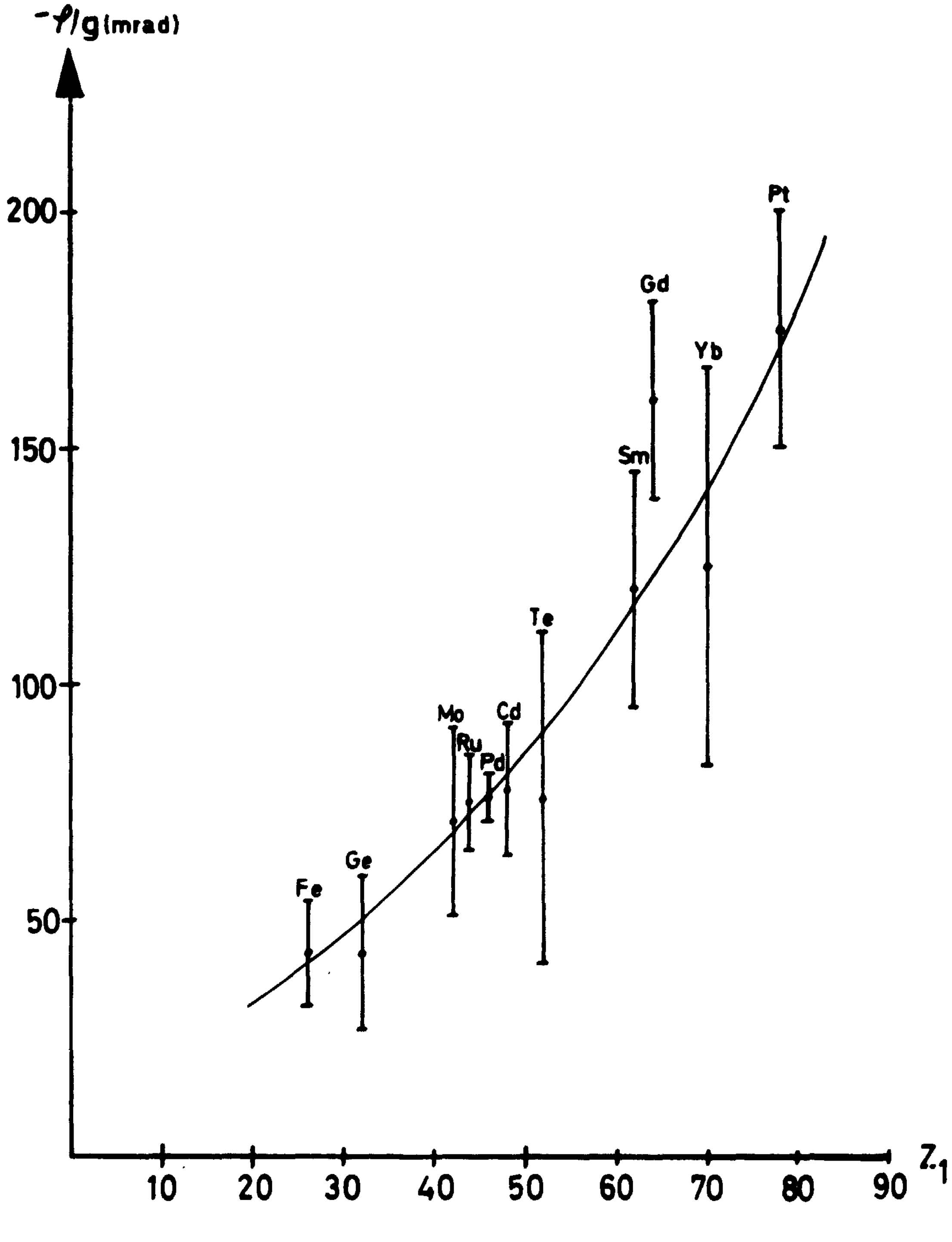
-φ/g (mrad)
200
150
100
50
Pt
Gd
Yb
Sm
Te
Mo
Ru
Pd
Cd
Ge
Fe
10
20
30
40
50
60
70
80
90
Z_1

FIG 8

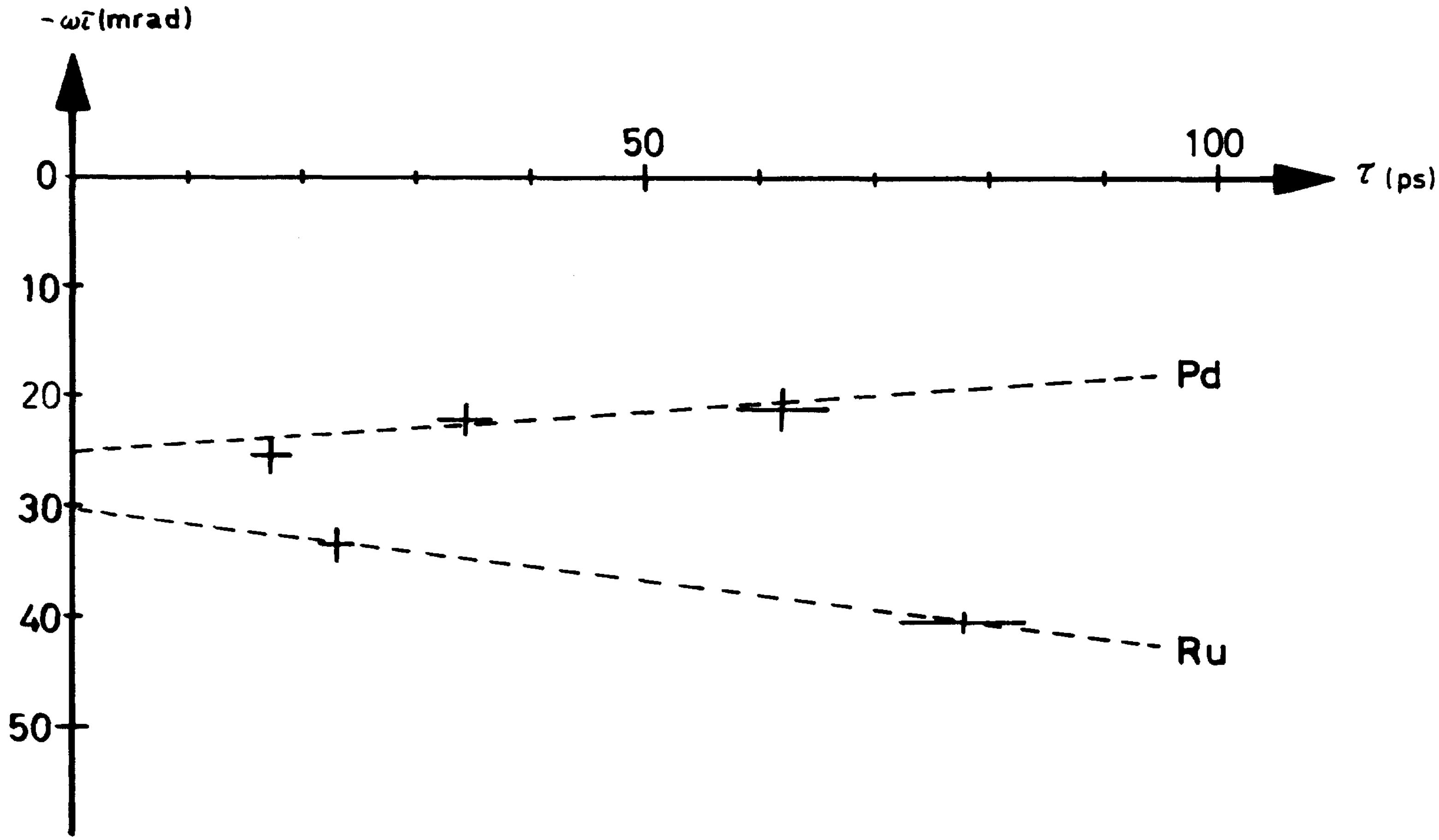

FIG 9

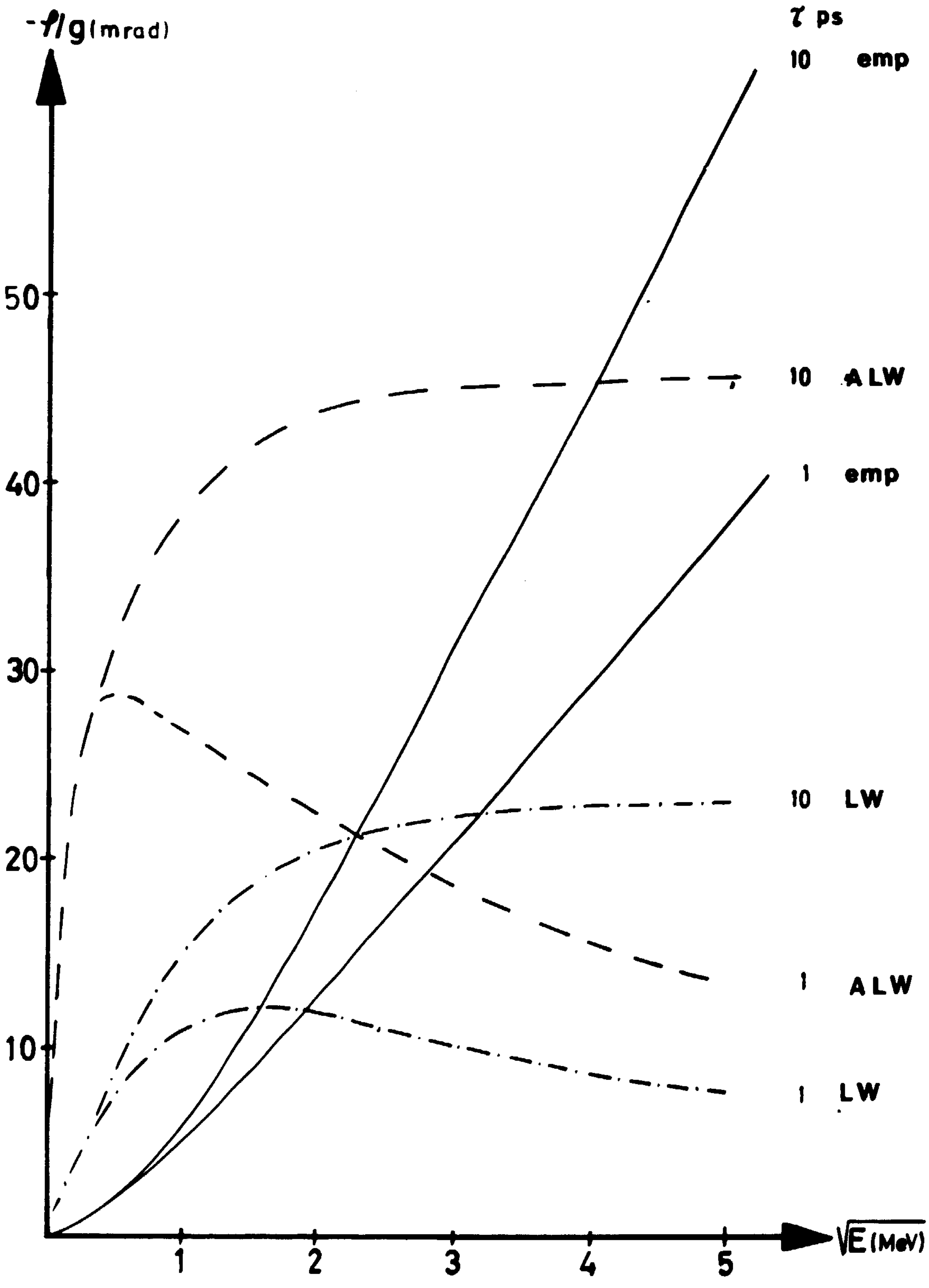
-f/g (mrad)
τ ps
10 emp
10 ALW
1 emp
10 LW
1 ALW
1 LW
50
40
30
20
10
1
2
3
4
5
√E (MeV)

FIG 10

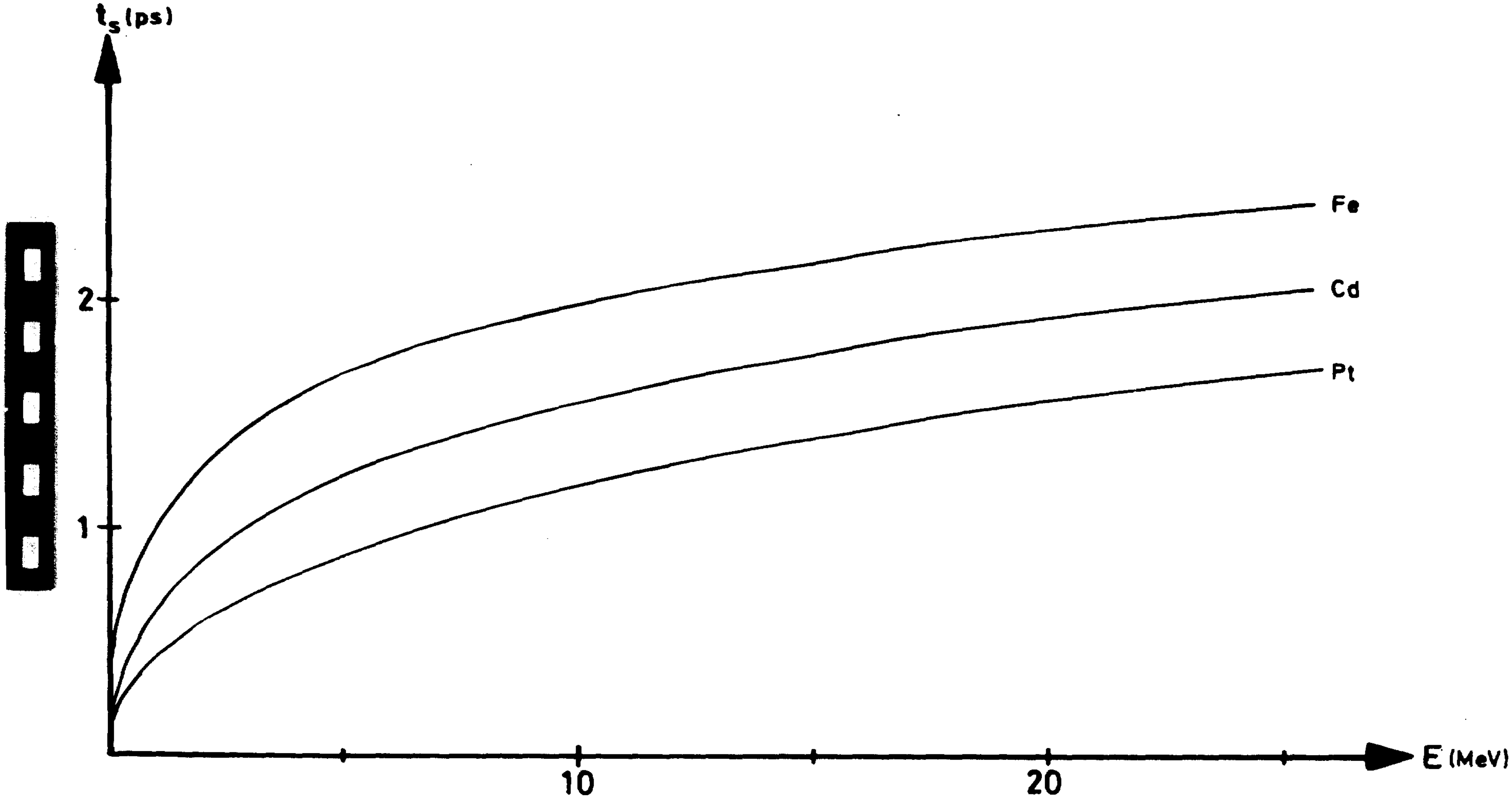

FIG 11